Monopoles for Microwave Catheter Ablation of Heart Tissue

S. Labonté, H.O. Ali, L. Roy
Electrical Engineering, University of Ottawa 161 Louis Pasteur, Ottawa, Ontario, Canada, K1N 6N5

Abstract— **The finite-element method is applied to the study of monopole antennas for microwave catheter ablation. Three geometries are considered: open-tip, dielectric-tip and metal-tip. Calculations are made for the magnetic field, the reflection coefficient and the power deposition pattern of the antennas immersed in normal saline. The theoretical results agree with measurements performed on prototypes. The differences between the antennas suggest that the metal-tip monopole best fulfills the requirements of catheter ablation of the endocardium. Optimal dimensions for a metal-tip monopole are also presented.**

Introduction

Catheter ablation is a medical procedure introduced in the mid-80's for the treatment of cardiac arrhythmias. The procedure involves burning the site of origin of the arrhythmia with the flow of an electrical current. The energy is delivered with a catheter advanced into the heart chamber. Radio-frequency (500–1000 kHz) electrical current has been used with great success for ablation of supra-ventricular arrhythmias. However, similar success was not achieved for ventricular tachycardias, partly due to the limited extent of radio-frequency (RF) lesions [1]. The use of microwave instead of RF energy is potentially more effective in achieving larger lesions due to its radiant nature. Wonnell *et al* [2] investigated a helical antenna operating at 2.45 GHz for this application. Their results suggest that the volume heated by microwave ablation can be several times larger than with conventional RF ablation. However, the size of their helical antenna is too large (length 9.5 mm, diameter 3.24 mm) for practical use. A possible alternative is to use a monopole antenna made by stripping the outer conductor at the end of a coaxial cable [3]. An analytical study of monopoles in lossy media was published recently, but the limitations of the model did not permit an optimization of the antenna dimensions [4]. Experiments by Rosenbaum *et al* [5] with monopole antennas and in-vitro and in-vivo models led to the conclusion that the microwave applicators they used are not capable of producing lesions larger than RF catheters. This work however provided few details about the geometry of their catheters and no theoretical analysis to substantiate their experimental results.

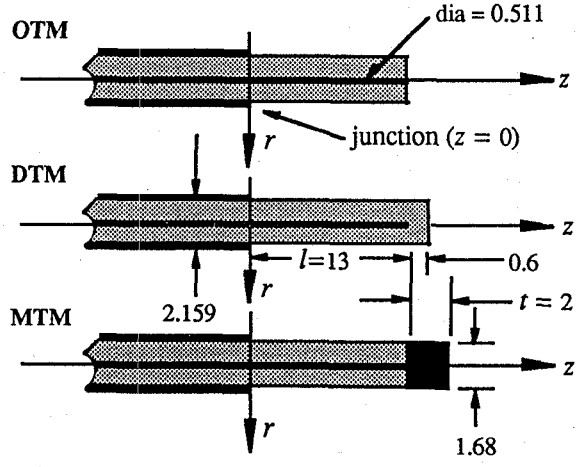

Figure 1: Monopole antennas. Dimensions in mm.

Monopole antennas have been studied extensively for hyperthermia applications [3] but none of the resulting designs is directly applicable to catheter ablation due to their large size. Specifically, antennas for microwave catheter ablation should 1) possess exposed metallic parts to record electrograms of the heart, 2) present low return loss to avoid excessive heating of the coaxial feed-line, 3) have a uniform heating pattern and 4) conform well to the catheter for easy catheterization.

In this paper, the finite-element method is used to study monopole antennas according to the above criteria. The work is in two parts. First, we study three different monopole geometries: 1) the open-tip monopole (OTM) where the extremity of the inner conductor is in contact with the ambient medium, 2) the dielectric-tip monopole (DTM) which is completely enclosed by the dielectric, and 3) the metal-tip monopole (MTM) which provides increased electrical contact with the tissue (Fig. 1). Numerical results for the reflection coefficient and the heating pattern of the antennas immersed in normal saline are presented. The accuracy of the numerical results is confirmed by measuring the reflection coefficient of antenna prototypes. The results reveal that the MTM offers the best compromise

TU 4E

CH3577-4/95/0000-0303$01.00 © 1995 IEEE

for catheter ablation. In the second part of this work, the dimensions of a MTM are optimized using finite-element modeling.

Finite Element Modeling

The antennas are assumed to be immersed in a homogeneous medium so that axial symmetry obtains ($\partial/\partial\phi = 0$) and the problem reduces to 2 dimensions. The modes of propagation are TM to z, and the only existing field components are E_r, E_z and H_ϕ. Eliminating the electric field from Maxwell's curl equations we obtain the following expression for H_ϕ in cylindrical coordinates:

$$-\frac{\partial}{\partial z}\left(\frac{\partial H_\phi}{\partial z}\right) - \frac{\partial}{\partial r}\left(\frac{1}{r}\frac{\partial}{\partial r}(rH_\phi)\right) = \omega^2\mu\epsilon H_\phi \quad (1)$$

where the usual notation is used and $\epsilon = \epsilon_0\epsilon_r - j\sigma/\omega$. Following this, H_ϕ is expressed in terms of known basis functions and Galerkin's procedure is used to transform (1) into a set of linear algebraic equations as is customary with the finite element method [6]. Note that this formulation in terms of H_ϕ is advantageous compared to that in terms of rH_ϕ especially for the number and complexity of the integrals which need to be solved [7].

Along the z-axis (Fig. 2), $H_\phi = 0$ because of symmetry. On the inner and outer conductors of the coaxial cable, the tangential E-field is zero. A TEM radiation condition is enforced on the outer boundary [6]. Finally, in the feeding coaxial cable a TEM mode is assumed so that $\partial H_\phi/\partial z = -jkH_\phi$ where k is the propagation constant inside the cable. The feed-boundary is located at $z = -29$ mm which ensures that higher-order modes reflected by the antenna junction have decayed to insignificant magnitudes [7]. The solution domain is discretized into roughly 10000 triangular elements with linear interpolatory functions.

Once $H_\phi(r, z)$ is calculated, it can be decomposed into incident and reflected waves at the feed-boundary. This information is used to calculate the voltage reflection coefficient (S_{11}) of the antenna. The E-field is derived from

$$E_r = \frac{-1}{j\omega\epsilon}\frac{\partial H_\phi}{\partial z}, \quad (2)$$

$$E_z = \frac{1}{j\omega\epsilon}\left(\frac{1}{r}\frac{\partial}{\partial r}rH_\phi\right) \quad (3)$$

using finite-difference approximations. Finally the SAR is obtained with

$$\mathrm{SAR} = \frac{\sigma}{2}\left(|E_r|^2 + |E_z|^2\right). \quad (4)$$

In the simulations we assume that the medium surrounding the antenna has the frequency dependent properties of normal saline [8]. The reason for this is that the properties of cardiac tissue are not known accurately and vary considerably between individuals. Normal saline is well characterized, with properties comparable to those of heart tissue, and constitutes a convenient standard.

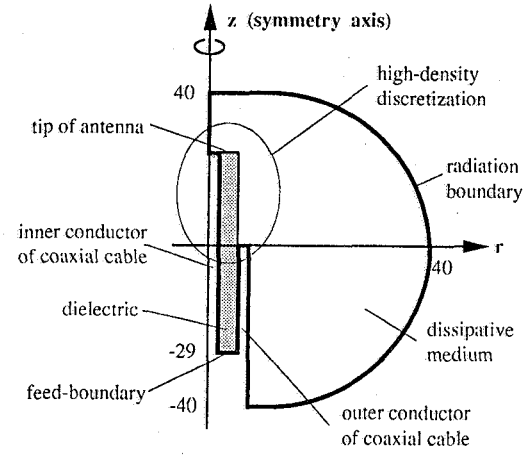

Figure 2: Solution domain of FEM computation. The open-tip monopole is shown. Not to scale.

Part I: Modeling of Monopoles

The three monopole geometries shown in Fig. 1 are modeled with the finite-element method. To verify the numerical results, reflection coefficient measurements are carried out on the OTM and MTM antennas. The prototypes are made by stripping the outer conductor of a 0.085 in. (2.159 mm) 50-Ω semi-rigid coaxial cable according to the dimensions shown in Fig. 1. The metal tip is fabricated with a short section of 1/16 in. (0.0625 mm) brass tubing, soldered to the inner conductor. The antennas have a total length of 160 mm with associated cable losses of 0.4 dB. Measurements are performed with the antennas immersed in 0.9% saline at room temperature. To eliminate the effect of the saline-air interface, the antennas are positioned at least 35 mm below the surface.

Fig. 3 displays the magnitude of H_ϕ calculated around the three antennas at a frequency of 2.45 GHz and an input voltage of 1 V (peak). The field is zero at the tip of the DTM and increases towards the junction ($z = 0$). It is similar but more uniform along the OTM. The MTM displays a minimum of the field at the junction and a maximum at the tip.

The calculated reflection coefficients as a function of frequency are presented in Fig. 4. Curves for the

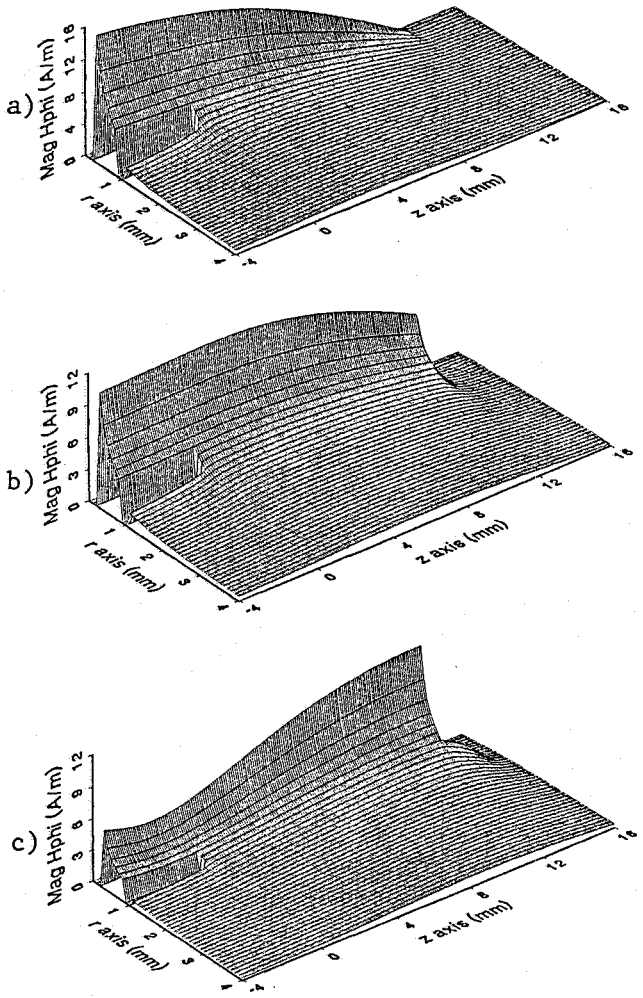

Figure 3: Magnitude of H_ϕ around the monopoles. The inner and outer conductors of the coaxial cable are at $r = 0$ and $r = 1$ respectively. a) DTM, b) OTM, c) MTM.

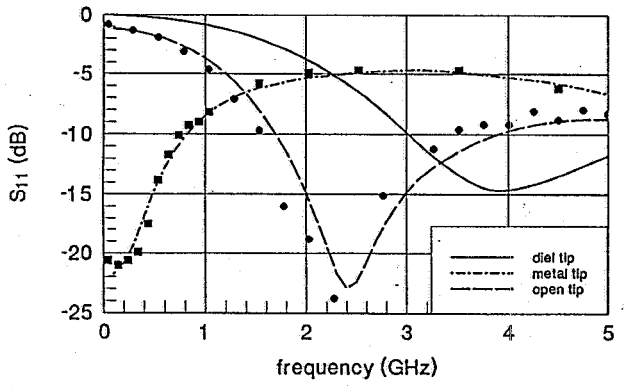

Figure 4: Magnitude of the reflection coefficients for the three antennas. The continuous curves are theoretical, the discrete points are experimental values.

three antennas are presented. Also on the same plot are the experimental results for the OTM and MTM. Corrections have been made to the measurements to remove the effect of cable losses. Good agreement is obtained between the calculated and measured values over a wide frequency range, validating the theoretical model. The 13 mm OTM exhibits a low value of S_{11} at 2.45 GHz. The MTM is well matched at low frequencies but has a high S_{11} of -5 dB at 2.45 GHz. The theoretical curve for the DTM presents a wide minimum at 4 GHz comparable to that measured on similar antennas in [3].

Normalized Specific Absorption Rate (SAR) patterns for the three antennas (not shown) reveal that the longitudinal SAR distributions differ significantly from one antenna to the other. The DTM has a highly concentrated SAR near the junction and very much less at the tip. The MTM has a more uniform distribution with a wide maximum around the tip. The OTM displays intermediate characteristics.

These results suggest that the MTM offers the best compromise for catheter ablation due to its relatively uniform heating pattern, acceptable S_{11} and exposed metallic tip allowing measurement of electrograms. In the following section, the dimensions of a MTM is optimized using finite element modeling.

Part II: Optimization of MTM

Two parameters of the antenna, the length of the exposed dielectric (l) and the length of the metallic tip (t) are varied so as to observe their effect on the S_{11} and the SAR. Two designs appear promising because of their relatively low reflection coefficient (Fig. 5) and uniform heating pattern (Figs. 6 and 7). The first has l =13 mm and t =2 mm and presents a return loss of 6 dB at 2.45 GHz. The second having l = 6.5 mm and t = 4 mm provides a return loss of 8 dB. Experiments on artificial and animal tissues remain to be performed in order to determine which of the two alternatives is superior.

Conclusion

Various designs for monopole antennas were analyzed using the finite-element method. Calculations for the reflection coefficient as a function of frequency agree well with measurements performed in normal saline. The analyses reveal that the metal-tip monopole exhibits a fairly uniform SAR along its length. This is due to the antenna current which is at a maximum near the tip. The optimization has led to two potential designs which exhibit satisfactory heating patterns and return loss. Performance in the

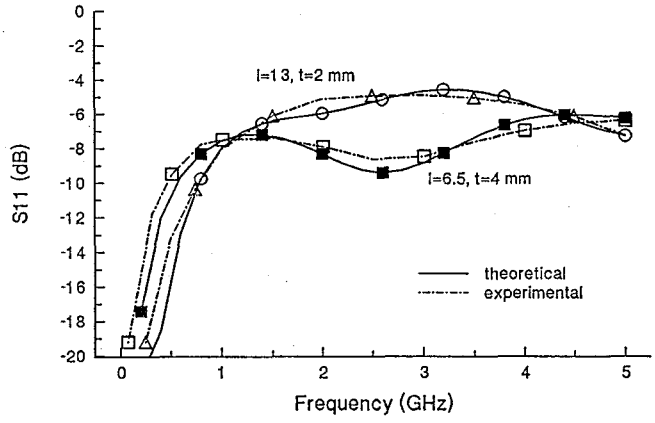

Figure 5: Theoretical and experimental reflection coefficient for the metal-tip monopoles. a) $l = 13$, $t = 2$. b) $l = 6.5$, $t = 4$. The dashed curves are experimental.

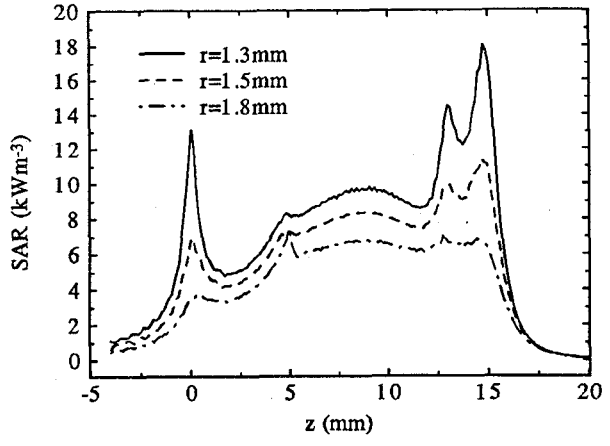

Figure 6: Heating patterns (W m^{-3}) for the MTM ($l = 13$, $t = 2$) along the z axis and at 3 r values. The values are divided by $(1 - |S_{11}|^2)$.

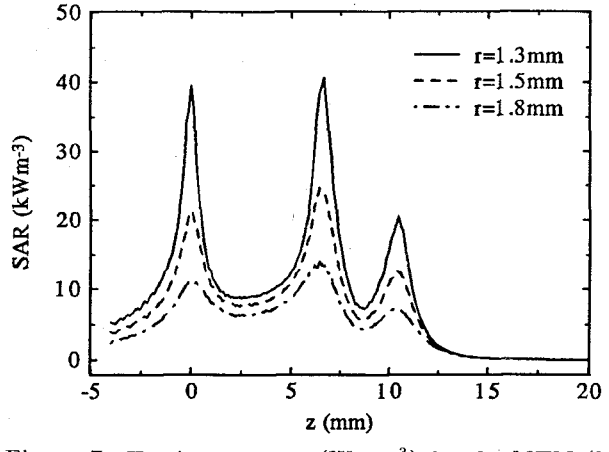

Figure 7: Heating patterns (W m^{-3}) for the MTM ($l = 6.5$, $t = 4$) along the z axis and at 3 r values. The values are divided by $(1 - |S_{11}|^2)$.

presence of heart tissues remains to be assessed. Microwave catheter ablation with these antennas may result in improved treatment of ventricular arrhythmias.

Acknowledgments

This research is supported in part by the Natural Sciences and Engineering Research Council of Canada. The authors thank Miss Marie-Aline Fabert and Mr. Martin Lee for conducting the computer simulations and fabricating the antenna prototypes.

References

[1] Newman D., Evans G.T., Scheinman M.M., "Catheter Ablation of Cardiac Arrhythmias," *Curr Probl Cardiol*, Vol. 14, no. 3, pp. 117-164, March 1989.

[2] Wonnell T.L., Stauffer P.R., Langberg J.J., "Evaluation of Microwave and Radio-Frequency Catheter Ablation in a Myocardium-Equivalent Phantom Material," *IEEE Trans Biomed Eng*, Vol. 39, No. 10, Oct. 1992, pp. 1086-1095.

[3] Iskander M.F., Tumeh A.M., "Design Optimization of Interstitial Antennas", *IEEE Trans Biomed Eng*, Vol. 36, No. 2, pp 238-246, Feb. 1989.

[4] Cerri G., DeLeo R., Primiani V.M., "Thermic End-Fire Interstitial Applicator for Microwave Hyperthermia," *IEEE T-MTT*, Vol. 41, No. 6/7, June/July 1993, pp. 1135–1142.

[5] Rosenbaum R.M., Greenspon A.J., Hsu S., Walinsky P., Rosen A., "RF and microwave ablation for the treatment of ventricular tachycardia," IEEE MTT-S Digest, Atlanta, pp. 1155-1158, 1993.

[6] Sumbar E., Vermeulen F.E., Chute F.S., "Implementation of Radiation Boundary Conditions in the Finite Element Analysis of Electromagnetic Wave Propagation," *IEEE Trans Microwave Theory Tech* Vol. 39, pp. 267-273, 1991.

[7] Maloney J.G., Smith G.S., Scott W.R., "Accurate Computation of the Radiation from Simple Antennas Using the Finite-Difference Time-Domain Method," *IEEE Trans Antennas Propagat*, Vol. 38, pp. 1059-1068, July 1990.

[8] Nyshadam A., Sibbald C.L., Stuchly S.S., "Permittivity Measurements Using Open-Ended Sensors and Reference Liquid Calibration: An Uncertainty Analysis," *IEEE Trans Microwave Theory Tech*, Vol. 40, No. 2, Feb. 1992, pp. 305-314.